Asian Journal of Atmospheric Environment
Vol. 8-3, pp. 154-161, September 2014
doi: http://dx.doi.org/10.5572/ajae.2014.8.3.154

# Chemical Properties of the Individual Asian Dust Particles Clarified by Micro-PIXE Analytical System

**Chang-Jin Ma*, Gong-Unn Kang[1)], Mikio Kasahara[2)] and Susumu Tohno[2)]**

Department of Environmental Science, Fukuoka Women's University, Fukuoka 813-8529, Japan
[1)]Department of Medical Administration, WonKwang Health Science University, Iksan 570-750 Korea
[2)]Graduate School of Energy Science, Kyoto University, Kyoto 606-8501, Japan

*Corresponding author. Tel: +81-92-661-2411, E-mail: ma@fwu.ac.jp

## ABSTRACT

The present study was undertaken to evaluate the chemical characteristics of Asian dust (hereafter called "AD") particles with the aid of the most advanced micro-PIXE (Particle-induced X-ray emission) analytical technique. To this end, size-selected particles were sampled on a rural peninsula of Korea (Byunsan, 35.37N; 126.27E) during AD and non-AD periods in 2004. The coarse particle ($>2\ \mu m$) number density during an AD event were 170 times higher than those of the non-AD counterpart. The average net-count of silica in individual particles collected on AD event was roughly 11 times higher than that of non-AD counterpart. The X-ray net-counts of trace elements (Zn, Co, Mn, and V) were also considerably high in AD relative to the non-AD day. Particle classification based on the inter ratio analysis of elemental net-count suggests that a large portion of the coarse particles collected during AD event underwent chemical transformation to a certain degree. The visual interpretation of micro-PIXE elemental maps and elemental localization data in and/or on individual AD particles clarified the internal mixture of AD particles with sea-salt and artificial metallic particles.

**Key words:** Asian dust, Aging, Individual particle, Long-range transport, Micro-PIXE

## 1. INTRODUCTION

The processes of chemical transformation (generally called aging) of mineral particles have been the long-term objective of AD studies. During long-range transport from the source region to the receptor areas (e.g., the Korean Peninsula, the Japanese islands, and the Pacific Ocean, and West/North America), AD particles experienced diverse aging processes such as the capturing of gases, coagulating of solid particles, cloud processing, and heterogeneous reactions. These aging processes permit the mixing of secondary species (e.g., sulphate, nitrate, and hydrochloric acid), sea salt, and biomass burning particles with the interior matter of AD particles (Ma, 2010; Hwang *et al*., 2008; Clarke *et al*., 2004; Zang *et al*., 2000).

As AD particles passed through clouds, the liquid phase oxidation of $SO_2$ could have potentially led to sulfate enrichment on the particle surface (Wurzler *et al*., 2000). This in turn can efficiently produce cloud condensation nuclei (CCN) and modify the amount and acidity of precipitation (Zhao *et al*., 2000), while such processes can also alter the marine ecosystem and radiative properties of dust clouds (Zhang and Iwasaka, 2004). In addition, it may ultimately negatively impact human health in a number of aspects.

In order to thoroughly understand these denaturations of AD particles, a detailed knowledge is desirable to precisely describe how man-made pollutants and sea-salt aerosol interact with natural individual AD particles. Zhang and Iwasaka (1998) carried out the study on the morphological and chemical composition of individual AD particles using the Scanning Electron Microscopy coupled with Energy Dispersive X-ray (SEM-EDX). Meanwhile, Kim and Ro (2010) introduced the low-Z EPMA (particle electron probe X-ray microanalysis) and they estimated the physicochemical properties and origins of individual AD particles.

In this study, in order to clarify the aging of AD particles, the micro-PIXE system was applied to the elemental analysis of the individual particles collected during AD and non-AD periods at a ground-based on the west coast of Korean peninsula.

## 2. MATERIAL AND METHODS

### 2.1 Sampling of Size-selected Particles

Byunsan peninsula (35.37N; 126.27E) of Korea was

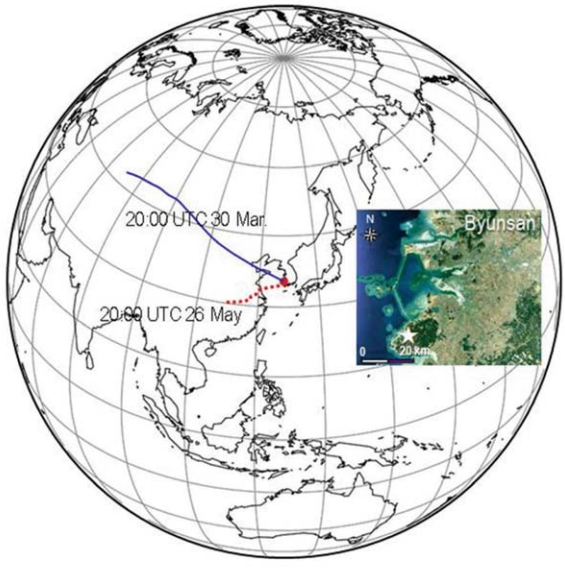


**Fig. 1.** Backward trajectories at 20 UTC 30 Mar., 2004 (a solid line) and at 20 UTC 26 May, 2004 (a dotted line) drawn by the METEX (Meteorological Data Explorer) model. Source point and the start height of air parcel were 35.37°N; 126.27 °E and 3000 m, respectively. Map of the Inside of model result shows the sampling location (the empty star) of Byunsan Peninsula.

selected as the sampling site of size-selected particles (Fig. 1). Because of its closeness to China, this site, marked by an empty star in Fig. 1, is a well suited area to measure AD.

An Andersen air sampler (Tokyo Dylec Co., LP-20-RS) with rearranged stages was employed in the sampling of size-selected particles. In a previous study, Chun *et al.* (2001) reported that the time temporal variation of aerosol number concentrations in Anmyon Island located on the west coast of Korea during AD period showed a considerable increase in the range of 3.67 μm to 6.06 μm. Particles were therefore classified into the cutoff diameter of two-size steps, i.e., the 2nd stage with 5.07 μm and the 3rd stage with 3.45 μm. The particle sampling was intensively carried out during AD event (Mar. 30, 2004) and non-AD day (May 26, 2004), respectively. In order to avoid a severe particle overlapping which obscures the chemical determination of particle-to-particle variations, the duration of sampling was adjusted to 20 minutes (the 3rd stage) and 30 minutes (the 2nd stage). After sample collection, every sample was placed in a clean sterilized petridish, which were sealed with Teflon tape and wrapped with aluminum foil. Every sample was placed in a cold storage bag during air transportation.

On AD and non-AD field campaign days, the wind speed ranges were 2.1-7.8 m $s^{-1}$ and 1.2-4.3 m $s^{-1}$, respectively and it was generally from the west. The backward wind trajectory projection (solid line in Fig. 1) at 20 UTC 30 Mar., 2004 was made using the METEX model and shows that the air parcel movement from the AD source regions to the receptor site (Byunsan). The temperatures of AD and non-AD days were around 3.0-12.9°C and 16.7-27.2°C, respectively.

## 2. 2 Particle Number Counting by an OPC

The number-size distribution of particles was monitored using an optical particle counter (OPC) (RION, KC-01D) during both AD and non-AD periods. The OPC was operated every 15 min in the dynamic range of $>0.3$ μm with five-step cutoff diameter of 0.3-0.5 μm, 0.5-1.0 μm, 1.0-2.0 μm, 2.0-5.0 μm, and $>5$ μm. The flow rate for the OPC was $3 \times 10^{-2}$ $m^3$ $hr^{-1}$. The accuracy of the OPC's sizing was checked by manufacturer (RION) as follows. Four-step known size monodisperse polystyrene type latex (PSL) spheres (0.294 μm, 0.505 μm, 1.001 μm, 2.106 μm) were employed. The PSL particle sizes are traceable to National Institute of Standards and Technology USA (NIST). The PSL was mixed with filtered air in the mixing chamber. Though the shapes of ambient particles, especially those of dust particles, are quite different from the PSL spheres, the OPC sizing accuracy check was conducted by sampling of PSL particles.

## 2. 3 Elemental Specification of Individual Particles by Micro-PIXE

In the present study, the micro-PIXE system equipped at the facilities of the Takasaki Ion Accelerators for Advanced Radiation Application in Japan atomic energy research institute was applied to the micro-scale elemental specification of individual particles (Fig. 2).

Microbeam PIXE, often called micro-PIXE, is a variation of PIXE that has become very important in recent years. It is a combination of the microbeam technique with PIXE analysis and in principle is analogous to the electron microprobe. Micro-PIXE is one of the most powerful micro-analytical techniques. Its greatest advantages are excellent sensitivity and the absolutely low detection limits ($10^{-15}$-$10^{-16}$ g). Also it has the merit of being a multielement non-destructive technique with a wide range of elements for various samples (Johansson *et al.*, 1995; Johansson and Campbell, 1988).

The micro-PIXE analysis is commonly performed as follows: Jumping of an electron in inner shell by the interaction with a particle beam − Moving of another electron in outer shell to an inner orbit − Emitting of a characteristic X-ray that has particular energy − Quantifying of elements by counting the number of characteristic X-rays. In this study, a 2.5 MeV $H^+$ microbeam accelerated by a 3 MV single-end accelerator was em-

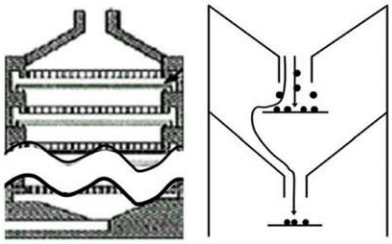

Size-resolved PM sampling
Andersen sampler (Tokyo Dylec Co.)

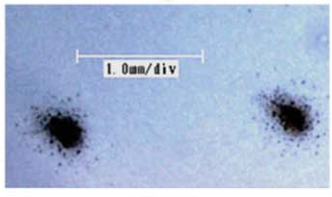


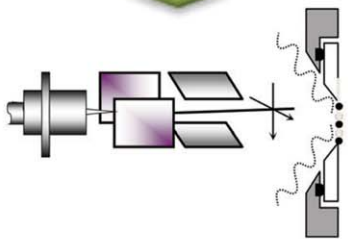

M-PIXE, Takasaki (IAARA)

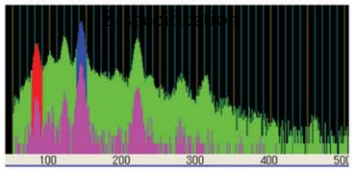


Z-specification

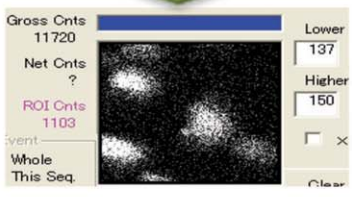


Z-micro distribution

**Fig. 2.** Flows of particle sampling and elemental analysis of individual AD particles.

ployed as a particle beam. Quantity of an element in a sample can be measured by counting the number of characteristic X-rays. The characteristic X-ray of element A can be calculated by following equation;

$$Y_A = N_A \times Q \times d\Omega \times E \times R_a \times \sigma^x \times 4\pi S^{-1}$$

where $N_A$ is the number of element A in sample, Q is the total number of incident particle, $d\Omega$ is a solid angle, E is detecting rate of detector, $R_a$ is the absorption rate of characteristic X-ray, $\sigma^x$ is a section area of characteristic X-ray generation, S is beam spot, respectively (Sakai *et al.*, 2005).

The more details of analytical processes and the novel double detector system of micro-PIXE employed in this study have been described elsewhere (Ma, 2010; Sakai *et al.*, 2005).

The file up of particles formed on a filter obscure individual particle analysis, i.e., the chemical determination of particle-to-particle variations. Therefore, in this study, the particles sparsely deposited around a spot (Fig. 2) were the target of micro-PIXE analysis. A total of 1000 particles collected in two intensive field measurements were quantitatively analyzed.

## 3. RESULTS AND DISCUSSION

### 3.1 Time Series Variation of Particle Number Concentration during AD Event and Non-AD Period

The number-size distributions of particles both larger than 2 μm and 0.3-2 μm were used for the comparison between AD and non-AD periods. Fig. 3 shows the time-series variation of particle number concentration and the ratio of AD to non-AD for the particles larger than 2 μm. In non-AD period, the particle number concentrations of both size fractions maintained a constant level, namely, 139,371-153,376 $L^{-1}$ in the size range between 0.3 μm and 2 μm and 245-300 $L^{-1}$ in the coarse particles larger than 2 μm. On the other hand, for small particles in the range of 0.3-2 μm collected during AD event, the particle number concentration fluctuated with small variations compared to that in non-AD period. However, the number of particles larger than 2 μm during AD event showed a very marked increase and was especially 170 times higher than in non-AD period at 17:00. This high number concentration of large particles was very noticeable especially during the day time. Although our data were limited at the case level, the particle number concentration obtained in our case study is in good agreement with that of early measurement in Seoul by Chun *et al.* (2001).

### 3.2 Net-counts of Major Elements in Individual Particles Collected in Each Field Campaign

Estimating the difference of elemental net-count between AD and non-AD is one of clear ways in deter-

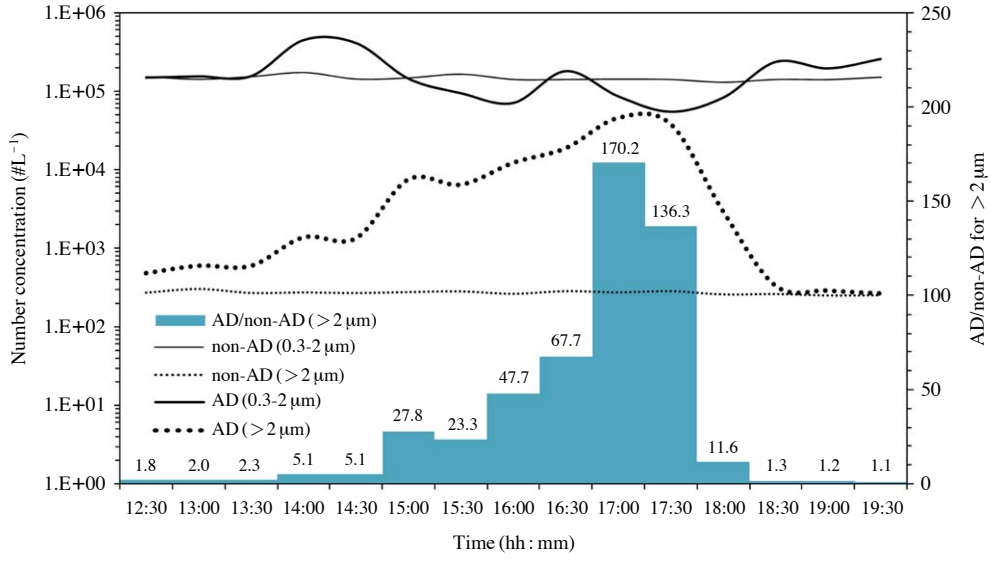


**Fig. 3.** Time series variation of particle number concentration and the ratio of AD to non-AD for $>2\,\mu m$.

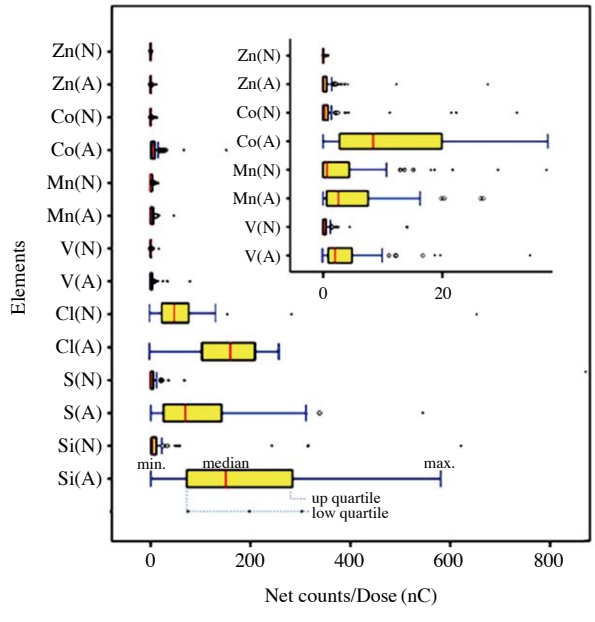


**Fig. 4.** Box plots of each elemental net-count of individual particles collected on AD event (A) and non-AD period (N), respectively.

mining high loading of pollutants in an AD event. The elements of interest (i.e., mineral, chloride, and trace elements) that are the most valuable for the estimation of the chemical modification of AD particles were selected. Fig. 4 shows the net-counts of major elements in individual particles collected in an AD event (A) and a non-AD day (N), respectively. In comparison to non-AD day, most of the elements show higher net-counts in the AD event. Representative silica, sulfur, and chloride on an AD event had marked and significantly higher net-counts. Among them, in particular, the average net-count silica in the AD event was roughly 11 times higher than that measured on a non-AD day. In addition, the net-counts of the minor elements (Zn, Co, Mn, and V) were also found to be definitely higher in an AD event relative to a non-AD day. This suggests that AD storm carried not only mineral dust, but also the dust captured and transported anthropogenic pollutants to the sampling site of the present study.

### 3.3 Particle Classifying by Comparing the Ratios of Elemental Net-counts of Micro-PIXE

In order to interpret the aging of individual coarse particles collected in the AD event, the ratios of X-ray net-counts among the three representative elements are presented in a ternary plot. Fig. 5 shows the ternary plot of the relative net-count ratios among S, Cl, and Ca in the individual particles collected during an AD event. From the ratios of atomic weight of S to that of Ca and the weight % of Cl and S in ocean, it was possible to classify the individual particles into two distinct groups. The particle group, which is formed on the border line ($S_{atomic\ weight} : Ca_{atomic\ weight} = 0.44 : 0.56$), probably contain $CaSO_4$ formed from the neutralization of $H_2SO_4$ by $CaCO_3$ (or $CaSO_4$ as natural mineral) accounts for a large portion of the total particles. Another possible process in the formation of $CaSO_4$ is the gas-to-particle conversion of $SO_x$ on the dust particle surface during transport in the air. The westerly pre-

vailing wind and the longitudinal mixing between air masses in accordance with the arrangement of high and low pressure systems contribute to the mixing processes among dust particles, sea-salt, and anthropogenic aerosol precursors (Song and Carmichael, 1999). Sea-salt aerosols can be classified into three categories (i.e., NaCl crystals, crystals of sulfates ($CaSO_4$ and $MgSO_4$), and chloride droplets ($MgCl_2$ and KCl)) (Andreae, 1986). It can therefore be assumed that this particle group has also relevance to the $CaSO_4$ particles produced by fractional crystallization of marine aerosol.

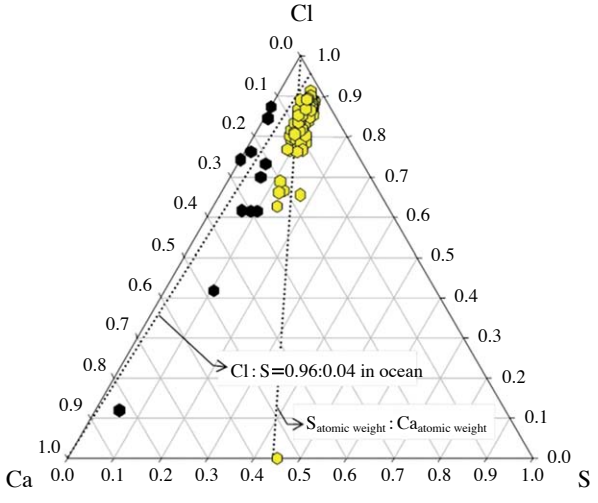


**Fig. 5.** Ternary plot of the relative net-count ratios among S, Cl, and Ca in individual particles collected during AD event.

The small portion of particles, which are marked as the bold hexagons near the line of Cl : S=0.96 : 0.04 in ocean (wt%), are presumably natural and transformed sea-salts.

### 3.4 Visual Interpretation of the X-ray Spectra, Elemental Maps, and Elemental Localization Data of Micro-PIXE for Individual AD Particles

From the scanning of microbeam on each individual particle, the particles in a whole selected portion (Fig. 6) could be classified into three distinct types. Fig. 6 shows the X-ray spectra drawn from three-type individual particles. The micro-PIXE spectra displayed in Fig. 6 shows a severe dissimilarity of elemental composition among individual coarse particles collected during our intensive field measurement. Particle-A shows the outstanding peaks for sea-salt components coexisted with soil-derived components such as Si, Al, K, and Ca. In the case of Particle-B, silica shows the most exclusive peak with several minor peaks (i.e., Cl, Na, Al, S, Mg, K, and Ca). These two types of particles are the typical example of internally mixed particles which contain both soil and marine components. Whereas, marine components without major crustal compositions such as Si and Al were detected in the Particle-C.

The aging of AD particles by sea-salt is discussed above (Fig. 5). Not only sea-salt, but many kinds of

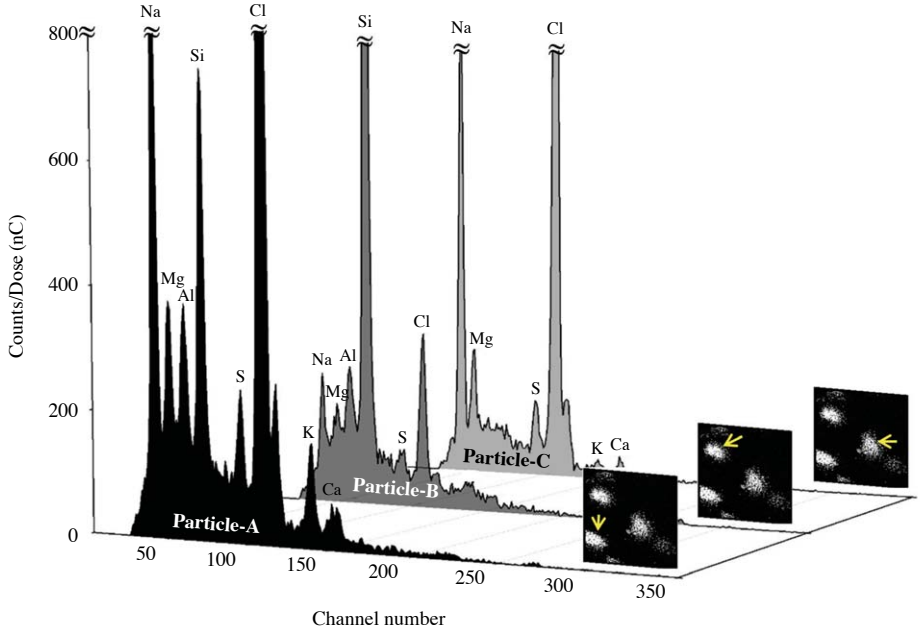


**Fig. 6.** X-ray spectra drawn from three-type individual particles collected during AD event.

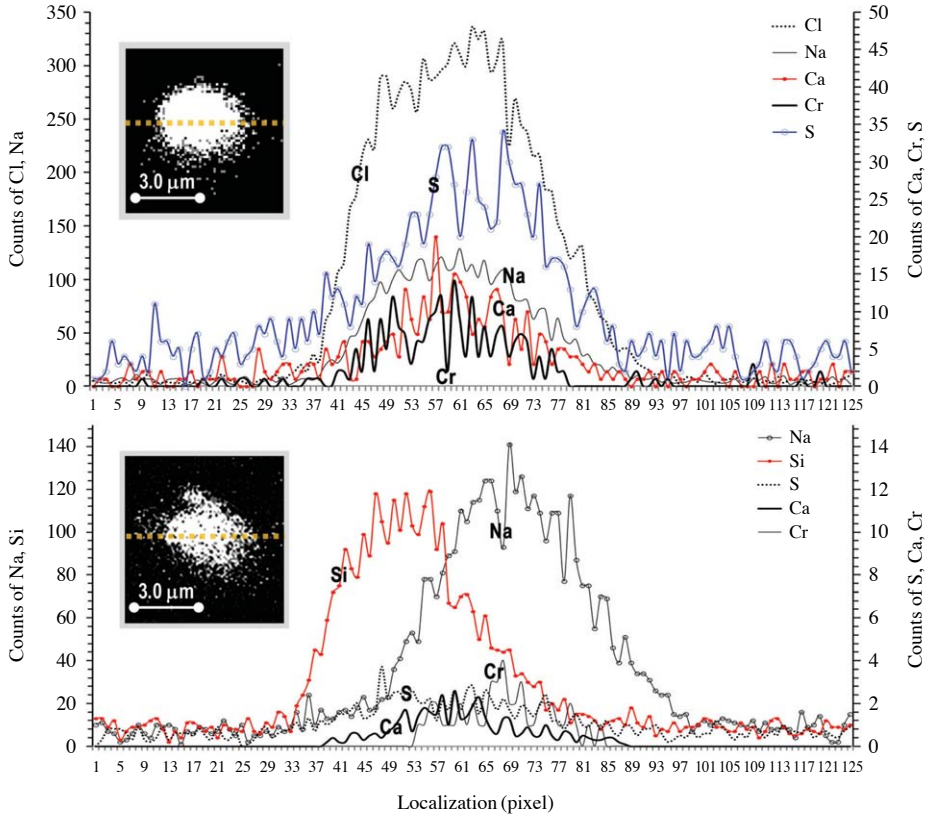


**Fig. 7.** The horizontal localization of several selected elements on the dotted line drawn in the center of two individual particles collected during AD event.

hazardous metallic components generated from small and large scaled coal combustion facilities including power station contribute to the chemical transformation of AD particles.

Here, an attempt was made to visually estimate both the internal mixing of AD particles with sea-salt and chromium, and their localization on and/or in individual AD particles. Fig. 7 shows the horizontal localization of several selected elements on the dotted line drawn in the center of two individual particles. The top particle in Fig. 7 shows a uniform mixture of several components (i.e., Cl, Na, Ca, Cr, and S). Meanwhile, the bottom particle shows an inhomogenity of elemental distribution, especially silica and sodium.

Although, Sino-Japan Friendship Centre for Environmental Protection (SJC) (2013) reported that the natural and the standard desert samples of China loess do not contain chromium, Ma *et al*. (2008), detected a small amount of chromium from the original sands collected at four different desert regions (i.e., Yinchuan, Wuwei, Dulan, and Yanchi) in China. Thus, it is desirable to investigate the origin of this chromium known as one of trace elements of coal combustion. The comparison of Cr/Ca between the original desert sand and the particle collected in AD event is good way to determine the source of chromium. The average mass ratio of Cr/Ca in the original desert sand (Ma *et al*., 2008) and the average net-count ratio of Cr/Ca in Fig. 7 are 0.012 and 0.341, respectively. This means the man-made chromium derived from the local sources in China was clearly adhered to AD particles during a long-range transport. This interior mixture of tiny metallic particles in AD particles is probably the result of several mechanisms, such as Brownian coagulation, impaction by differential sedimentation, and coalescence of cloud droplets containing AD particles with those containing metallic particles. The study on the health effects of the metals bound to AD particles conducted by Hong *et al*. (2010) suggested that the exposure of the AD particles containing metals reduces children's pulmonary function.

Together with the horizontal distribution of elemental intensity described in Fig. 7, the local area analysis of single particle allows us to precisely interpret the chemical inhomogenity of single particle. Fig. 8 shows the local inhomogenity of the elemental distribution on and/or the particle horizontally analyzed in Fig. 7.

Outer white and inner gray color spectra in Fig. 8

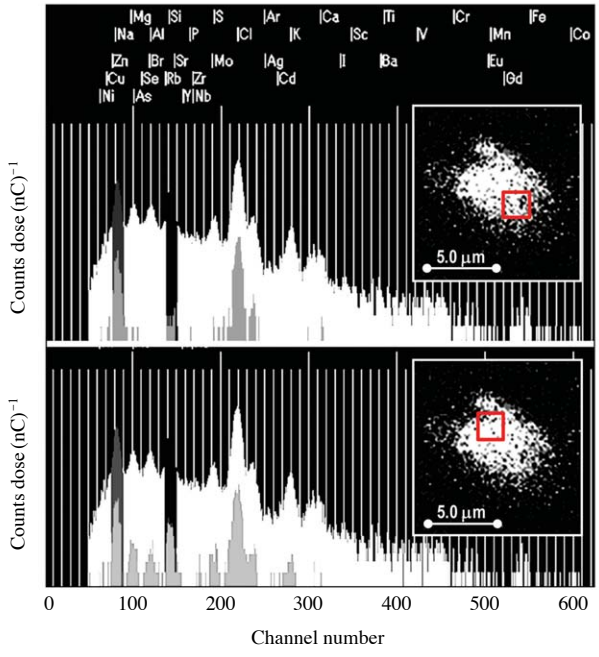


**Fig. 8.** Inhomogenity of the elemental distribution on and/or in the particle horizontally analyzed at the bottom of Fig. 7.

were formed by a microbeam scanning on the whole and each square portion of a particle, respectively. The top portion of particle contains enriched sea-salt with Si, Al, Mg, and K. However, sea-salt components were matchlessly detected in the bottom portion of particle. This heterogeneous elemental distribution agrees well with the result of Fig. 7.

On the basis of both X-ray spectra and elemental maps of micro-PIXE for the randomly selected individual particles collected during an AD event, the relative number fraction of each particle type was calculated. The non-aged particles (i.e., the sum of fresh sea-salt and mineral particles) account for 28.6%. Whereas, the chemically transformed particles account for 71.4 %. These internally mixed particles are moreover classified into three groups (i.e., Group-1 (sea-salt+mineral) with 17.1%, Group-2 (sea-salt+mineral+artificial metals (Co, Zn, and Cr)) with 28.6%, and Group-3 (sea-salt+artificial metals) with 25.7%). This result indicates that AD particles collected on the west coast of Korea tend to be effectively aged during their long-range transport.

## 4. CONCLUSIONS

A change in the chemical composition of AD particles is occurred by absorption of polluted ambient gases, coagulation of particles containing hazardous metallic components, and coalescence of cloud droplets during their long-range transport. This chemical transformation of AD particles can dramatically alter their optical properties, cloud-forming properties, and health effects. However, the modification processes of AD particles are still in doubt. In the present study, we made an attempt to clarify the aging of AD particles collected on the west coast of Korean Peninsula by means of the most advanced micro-PIXE analytical technique. Although the numerical limitation of particles that analyzed and discussed in the present study is apprehensive, the inter ratios of elemental net-count among S, Cl, and Ca obtained individual particle analysis suggest that AD particles were strongly affected by anthropogenic pollutants originating from the mainland China before arriving at the Byunsan Peninsula. The visual interpretation of X-ray spectra, elemental maps, and elemental localization data of micro-PIXE for individual AD particles was useful to evaluate the internal mixing state of individual AD particles with tiny metallic particles.

## ACKNOWLEDGEMENT

The authors wish to express thanks to all the members, especially Mr. T. Sakai, in the Advanced radiation technology center, Japan Atomic Energy Research Institute for their help of micro-PIXE analysis. The METEX program (http://db.cger.nies.go.jp/ metex/trajectory.html) for backward trajectory developed and provided by the National Institute for Environmental Studies, Japan was also helpful to data interpretation. This study was partially supported by funding from the Consortium of Asian Universities in Fukuoka (CAUFUK), Fukuoka Prefecture, Japan.

## REFERENCES

Andreae, M.O., Charlson, J.C., Bruynseels, F., Storms, H., Van Grieken, R., Maenhant, W. (1986) Internal mixture of sea salt, silicates and excess sulfate in marine aerosols. Science 232, 1620-1623.

Chun, Y.S., Kim, J.Y., Choi, J.C., Boo, K.O., Oh, S.N., Lee, M.H. (2001) Characteristic number size distribution of aerosol during Asian dust period in Korea. Atmospheric Environment 35, 2715-2721.

Clarke, A., Dhinozuka, Y., Kapustin, V.N., Howell, S., Huebert, B., Doherty, S., Anderson, T., Covert, D., Anderson, J., Hua, X., Moore, K.G., McNaughton, C., Carmichael, G., Weber, R. (2004) Size distributions and mixtures of dust and black carbon aerosol in Asian outflow: Physiochemistry and optical properties. Journal of Geophysical Research 109 (D15), doi:10.1029/2003

JD004378.
Hong, Y.C., Pan, X.C., Kim, S.Y., Park, K., Park, E.J., Jin, X., Yi, S.M., Kim, Y.H., Park, C.H., Song, S., Kim, H. (2010) Asian dust storm and pulmonary function of school children in Seoul. Science of the Total Environment 408(4), 754-759.
Hwang, H.J., Kim, H.K., Ro. C.U. (2008) Single-particle characterization of aerosol samples collected before and during an Asian dust storm in Chuncheon, Korea. Atmospheric Environment 42, 8738-874.
Johansson, S.A.E., Campbell, J.L. (1988) PIXE: A novel technique for elemental analysis. New York, John Wiley & Sons, pp. 134-140.
Johansson, S.A.E., Campbell, J.L., Malmqvist, K.G. (1995) Particle-Induced X-Ray Emission Spectrometry (PIXE), New York, John Wiley & Sons, pp. 111-120.
Kim, H.K., Ro, C.U. (2010) Characterization of individual atmospheric aerosols using quantitative energy dispersive-electron probe X-ray microanalysis. Asian Journal of Atmospheric Environment 4, 115-140.
Ma, C.J. (2010) Chemical transformation of individual Asian dust particles estimated by the novel double detector system of micro-PIXE. Asian Journal of Atmospheric Environment 4-2, 106-114.
Ma, C.J., Kasahara, M., Tohno, S., Kim, K.H. (2008) Physicochemical properties of Asian dust sources. Asian Journal of Atmospheric Environment 2, 26-33.
Sakai, T., Oikawa, M., Sato, T. (2005) External scanning proton microprobe -a new method for in-air elemental analysis. Journal of Nuclear and Radiochemical Sciences 6, 69-71.
Sino-Japan Friendship Centre for Environmental Protection (SJC) (2013) http://www.china-epc.cn/japan/index_e.htm.
Song, C.H., Carmichael, G.R. (1999) The aging process of naturally emitted aerosol (sea-salt and mineral aerosol) during long range transport. Atmospheric Environment 33, 2203-2218.
Wurzler, S., Reisin, T.G., Levin, Z. (2000) Modification of mineral dust particles by cloud processing and subsequent effects on drop size distributions. Journal of Geophysical Research 105, 4501-4512.
Zhang, D.J., Iwasaka, Y. (1998) Morphology and chemical composition of individual dust particles collected over Wakasa bay, Japan. Journal of Aerosol Science 29, S217-S218.
Zhang, D.J., Iwasaka, Y. (2004) Size change of Asian dust particles caused by sea salt interaction: Measurements in southwestern Japan. Journal of Geophysical Research 31, L15102, doi:10.1029/2004GL020087.
Zhang, D.Z., Iwasaka, Y., Shi, G.Y., Zang, J.Y., Matsuki, A., Trochkine, D. (2000) Mixture state and size of Asian dust particles collected at southwestern Japan in spring 2000. Journal of Geophysical Research 108 (D24), doi: 10.1029/ 2003JD003869.
Zhao, X., Wang, Z., Zhuang, G., Pang, C. (2000) Model study on the transport and mixing of dust aerosols and pollutants during an Asian dust storm in March 2002. Terrestrial Atmospheric and Oceanic Sciences 18, 437-457.

(Received 23 May 2014, revised 10 July 2014, accepted 5 August 2014)